Table I. Solubilities of Propane and Carbon Dioxide in Hexane, Heptane, Dodecane, and Hexadecane

Gas	Solvent	Temp, °C			
		25	35	45	
Propane	Hexane L	23.75			
	x	0.115			
	x	0.116 (*7*)			
	Heptane L	21.65	17.30	14.60	
	x	0.117	0.0942	0.0798	
	Dodecane L	14.95	12.24	10.21	
	x	0.123	0.101	0.0831	
	Hexadecane L	12.65	10.25	8.58	
	x	0.133	0.109	0.0896	
		10	25	40	50
Carbon dioxide	Heptane L	2.24	1.95	1.71	
	$(10^4)\,x$	139	117	99.5	
	$(10^4)\,x$		121 (*4*)		
	Dodecane L	1.55	1.37	1.22	
	$(10^4)\,x$	149	127	109	
	Hexadecane L		1.16	1.05	1.00
	$(10^4)\,x$		138	121	113

L = Ostwald coefficient; x = mole fraction.

other workers. The densities and vapor pressures (calculated from Antoine constants) were obtained from Rossini (*6*).

RESULTS

The solubilities of propane at 25°, 35°, and 45°C in heptane, dodecane, and hexadecane and of carbon dioxide at 10°, 25°, and 40°C in heptane and dodecane, and at 25°, 40°, and 50°C in hexadecane are reported in Table I both as Ostwald coefficients and mole fractions. The solubility of propane in hexane at 25°C was measured and compared with that of Thomsen and Gjaldbaek (*7*). A similar comparison was made for the solubility of carbon dioxide in heptane at 25°C with that of Gjaldbaek (*4*). Whereas the former comparison was very favorable (within 1%), the latter comparison was not (about 3% difference). Because Gjaldbaek described corrections for contamination of air in the carbon dioxide for his measurements, we considered the possibility for error in his reported results. Repeated attempts failed to reproduce the somewhat higher value.

ACKNOWLEDGMENT

The authors acknowledge with appreciation use of the University of Ottawa Computing Centre.

NOMENCLATURE

L = Ostwald coefficient
p_G = gas partial pressure, atm
P_t = total pressure, atm
S = solvent infusion rate, ml/min
v_G' = volume of dry gas absorbed, ml
v_G = equivalent volume of vapor saturated gas absorbed, ml
v_L = volume solvent, ml
v_S = volume solution, ml
V_G = gas molar volume at atmospheric pressure and temperature of experiment, ml/g mol
V_L = partial molal volume of dissolved gas in solntion, ml/g mol
x = mole fraction dissolved gas at partial pressure of 1 atm
θ = elapsed time of solubility experiment, min

LITERATURE CITED

(1) Battino, R., Clever, H. L., *Chem. Rev.*, **66**, 395 (1966).
(2) Din, F., "Thermodynamic Functions of Gases," Vol. 1, p 124, Butterworths, London, 1956.
(3) Din, F., *ibid.*, Vol. 2, p 136, 1962.
(4) Gjaldbaek, J. C., *Acta. Chem. Scand.*, **7**, 537 (1953).
(5) Hayduk, W., Cheng, S. C., *Can. J. Chem. Eng.*, **48**, 93 (1970).
(6) Rossini, F. D., et al., Am. Petroleum Inst. Res. Project 44, *Circ.*, Natl. Bur. Stand., 1947.
(7) Thomsen, E. S., Gjaldbaek, J. C., *Acta Chem. Scand.*, **17**, 134 (1963).

Received for review March 10, 1971. Accepted September 7, 1971. Work supported by an operating grant from the National Research Council of Canada.

Liquid-Solid Equilibria in the Na^+—$HCOO^-$, —CNS^-, —NO_3^- Ternary System

MARIA A. BERCHIESI, AUGUSTO CINGOLANI, and GIANFRANCESCO BERCHIESI[1]
Istituto Chimico, Università degli Studi, 62032 Camerino, Italy

Thermal analysis and differential scanning calorimetry were used to study solid-liquid equilibria in order to draw the polythermal projection of the ternary system Na^+—$HCOO^-$, —CNS^-, —NO_3^-. Five crystallization regions and three invariant points were identified.

Research on the molten salts systems showed the connections between polythermal projections of the systems and the thermodynamic or structural properties of the components. Outline of the K^+—$HCOO^-$, —CNS^-, —NO_3^- system was discussed previously (*1*). The present paper deals with the crystallization temperatures in the Na^+—$HCOO^-$, —CNS^-, —NO_3^- ternary system.

EXPERIMENTAL

The first crystallization temperatures of the melted mixtures were determined by a Chromel-Alumel thermocouple, checked by comparison with an NBS-certified Pt resistance thermometer, and connected with a Leeds & Northrup type K-5 potentiometer. The pyrex container of the melted mixtures was put in a furnace whose temperature was controlled by a second thermocouple, connected with a Leeds & Northrup

---

[1] To whom correspondence should be addressed.

CAT control unit. If a certain measurement had to be repeated, an auxiliary heater was used for a quick remelting. The details of this method were described elsewhere (*2, 5, 6*).

Whenever it was necessary to get more complete information, a differential scanning calorimeter DSC-IB Perkin-Elmer was used. In conventional DTA, the temperature difference between the sample and a reference body is measured throughout the analysis, while a DSC unit records the differential energy to be supplied for keeping both materials continously at the same temperature. The thermogram drawing-pen excursions (briefly called peaks) represent transitions occurring in the sample. The details and the calibration were described previously (*4*).

The composition of a ternary system was plotted on a equilateral triangle, and a right triangular prism represented the temperature-composition relationships. The faces of the prism represented the binary system. Generally the final results were given, or as a perspective projection (projection on the faces of the prism), or as polythermal projection (orthogonal projection on the composition plane) of the eutectic valleys. The polythermal projection was drawn by projecting on the base triangle the characteristic points of several sections of the prism (pseudobinary systems). The chemicals employed were high-purity C. Erba HCOONa and $NaNO_3$ and Merck NaCNS, of a purity not less than 99%. The melting points of the thoroughly dehydrated salts were: 257.5°C for HCOONa, 306.0°C for $NaNO_3$ and 307.5°C for NaCNS in agreement with previous measurements (*7, 10*).

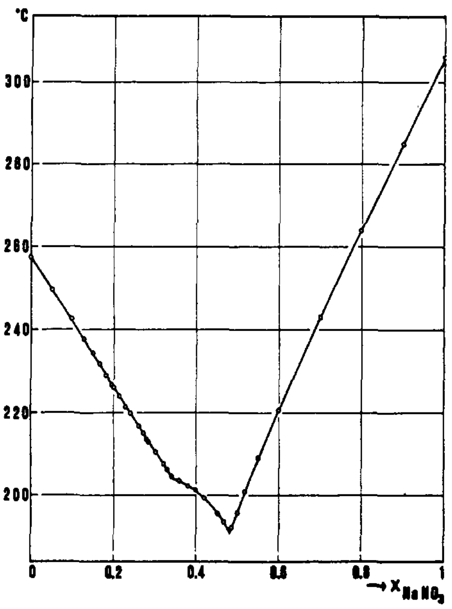

Figure 1. Liquid-solid equilibria in the $HCOONa-NaNO_3$ binary system

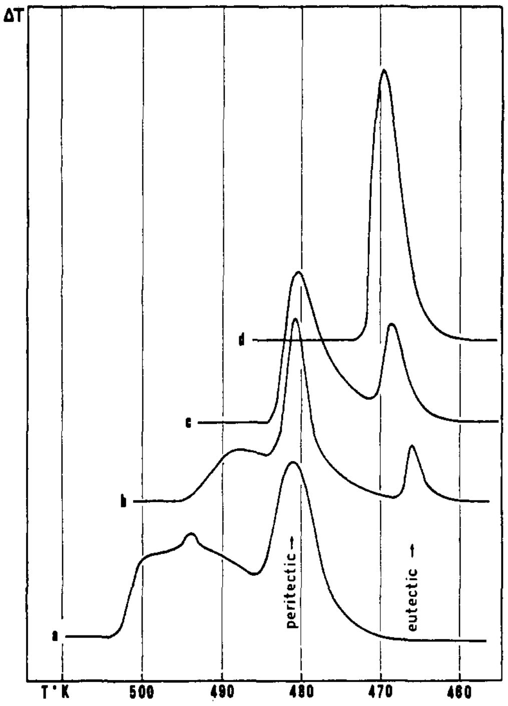

Figure 2. Thermograms of some mixtures of the $HCOONa-NaNO_3$ binary system

a. $X_{NaNO_3} = 0.2074$: peaks corresponding to the peritectic transition (204°C) and to the complete fusion
b. $X_{NaNO_3} = 0.2688$: peaks corresponding to the eutectic fusion (191°C), to the peritectic transition (204°C) and to the complete fusion
c. $_{NaNO_3} = 0.3440$: peaks corresponding to the eutectic fusion and to the peritectic transition
d. $X_{NaNO_3} = 0.4810$: peak corresponding to the eutectic fusion

RESULTS AND DISCUSSION

The $HCOONa-NaNO_3$ and $NaCNS-NaNO_3$ binary systems, concerning two sides of the system, were previously measured: the first by Sokolov (*11*) the second by Sinistri and Franzosini (*9*). In the $HCOONa-NaNO_3$ binary system Sokolov observed only a eutectic at 186°C and 49% of $NaNO_3$; we observe, however (Table I, Figure 1), a eutectic at 191°C and $X_{NaNO_3} = 0.481$ and a transition point at 204°C and $X_{NaNO_3} = 0.344$. The measurements were carried out several times with the utmost accuracy and we chose only those measurements that agreed within 1 $\mu V \simeq 0.03°C$. Some mixtures $HCOONa-NaNO_3$ were analyzed by a Perkin-Elmer differential scanning calorimeter DSC-IB, and thermograms of this system are reported in Figure 2. We observed in the concentration range $0 < X_{NaNO_3} < 0.344$ the usual peak (at 204°C) corresponding to the peritectic transition (Figure 2*a*,*b*,*c*). The peak belonging to eutectic fusion was apparent only in the concentration range $0.25 < X_{NaNO_3} < 1$ (Figure 2*b*,*c*,*d*). For this reason the molar fraction $X_{NaNO_3} = 0.25$ represented the last point where the eutectic fusion may occur, and the composition of the incongruently melting compound was $(X_{HCOONa}/X_{NaNO_3}) = (0.75/0.25) = 3:3$ $HCOONa.NaNO_3$. The agreement with Sinistri's data concerning the $NaCNS-NaNO_3$ system was satisfactory.

Table I. Liquidus Curve of Binary System $Na(HCOO,NO_3)$

X_{NaNO_3}	*t*, °C	X_{NaNO_3}	*t*, °C
0.0000	257.50	0.3307	205.85
0.0517	249.50	0.3399	204.50
0.0988	242.73	0.3598	203.50
0.1269	237.58	0.3809	202.13
0.1504	234.43	0.3999	201.25
0.1659	231.65	0.4201	199.25
0.1812	229.03	0.4496	195.38
0.1941	226.58	0.4661	193.50
0.2008	226.13	0.4857	192.10
0.2153	223.98	0.4993	195.75
0.2278	221.35	0.5167	200.87
0.2400	219.85	0.5509	208.93
0.2608	216.73	0.6001	220.70
0.2719	215.08	0.7002	243.03
0.2804	213.55	0.7990	263.95
0.2861	213.05	0.9004	284.98
0.3007	210.30	1.0000	306.00
0.3203	207.54		

In the system HCOONa-NaCNS measured by us and dis-

Table II. Characteristic Points of Internal Sections in Na^+—$HCOO^-$, —CNS^-, —NO_3^- Ternary System

Section	Composition of starting mixtures, moles		Added comp.	Characteristic points					
				x_{ac}[a]	T, °C	x_{ac}	T, °C	x_{ac}	T, °C
I	HCOONa + NaCNS	1.63:1	$NaNO_3$	0.325	166.5	. . .	. . .	. . .	. . .
II	HCOONa + NaCNS	2.23:1	$NaNO_3$	0.243	160.0	0.296	154.5	. . .	. . .
III	HCOONa + NaCNS	2.85:1	$NaNO_3$	0.227	170.5	0.343	166.5	. . .	. . .
IV	HCOONa + NaCNS	3.55:1	$NaNO_3$	0.245	175.5	0.370	172.5	. . .	. . .
V	HCOONa + NaCNS	8.99:1	$NaNO_3$	0.300	193.0	0.431	183.0	. . .	. . .
VI	HCOONa + $NaNO_3$	8.46:1	NaCNS	0.247	191.0	0.344	179.5	. . .	. . .
VII	HCOONa + $NaNO_3$	4.62:1	NaCNS	0.231	182.5	0.312	173.5	. . .	. . .
VIII	HCOONa + $NaNO_3$	3.17:1	NaCNS	0.215	174.0	0.292	167.5	. . .	. .
IX	HCOONa + $NaNO_3$	2.70:1	NaCNS	0.218	169.0	0.273	165.0	. . .	. . .
X	HCOONa + $NaNO_3$	2.29:1	NaCNS	0.136	180.5	0.232	162.5	0.258	160.0
XI	HCOONa + $NaNO_3$	1.86:1	NaCNS	0.241	156.0	. . .	. . .	. . .	. . .
XII	HCOONa + $NaNO_3$	1.76:1	NaCNS	0.235	154.5	. . .	. . .	. . .	. . .
XIII	HCOONa + $NaNO_3$	1.53:1	NaCNS	0.197	161.0	0.237	156.5	. . .	. . .
XIV	$NaNO_3$ + HCOONa	1.86:1	NaCNS	0.337	197.0	. . .	. . .	. . .	. . .

[a] Molar fraction of the added component.

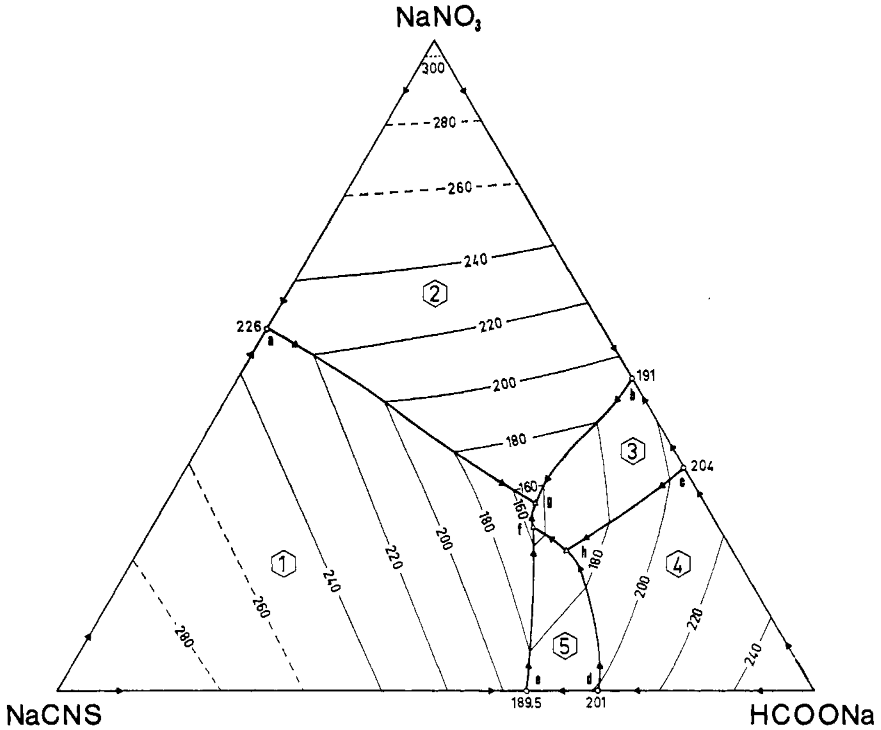

Figure 3. Polythermal projection of the ternary system Na^+—$HCOO^-$, —NO_3^-, —CNS^-

cussed in another note (*6*), we observed the eutectic at 185.5°C and $X_{NaCNS} = 0.380$ and a transition point at 200.8°C and $X_{NaCNS} = 0.286$. To draw the polythermal projection of the system, we measured the solid-liquid equilibria along 14 internal sections (*8*) whose characteristic points are reported in Table II. The five observed crystallization regions, the isothermal lines, and the projection of the eutectic valleys are shown in Figure 3. At higher temperature than 260°C, the ternary mixtures were thermally unstable (dashed isothermal lines in Figure 3). In the ternary system we observed three invariant points: two ternary transition points and a ternary eutectic, the composition of which (Table III) was determined by the perspective projections of the eutectic valleys into two sides (Figure 4) of the prism representative of the system. [The details of of this method are given in the cited book of Ricci (*8*).] Their melting temperatures were experimentally confirmed. The crystallization areas of the three salts and the two incongruently melting compounds expressed as percentage of the total composition triangle area, are:

Table III. Coordinates of Invariant Points

Point	Composition		T, °C
	X_{NaCNS}	X_{HCOONa}	
f	0.245	0.502	157.5
g	0.223	0.488	153.0
h	0.219	0.565	167.5

Crystallization region, °C	Liquidus area, %
1	44.70
2	32.78
3	5.30
4	13.63
5	3.60

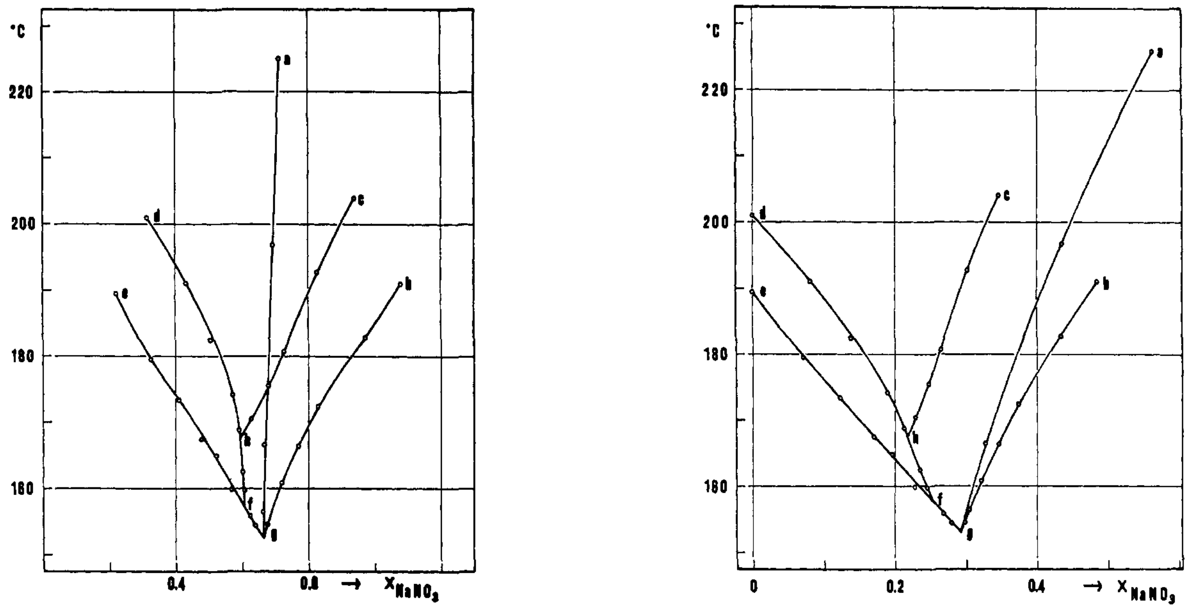

(a) (b)

Figure 4. Perspective projection of the eutectic valleys

a. On the NaCNS–NaNO$_3$ side
b. On a side perpendicular to the NaCNS–HCOONa side

The extent of the crystallization areas in a phase diagram depended generally on the melting temperature of the components (*2*). In the systems Na$^+$—CNS$^-$, —HCOO$^-$, —NO$_3^-$ and K$^+$—CNS$^-$, —HCOO$^-$, —NO$_3^-$ (*1*), the difference of the melting temperatures between NaCNS (mp 307°C) and NaNO$_3$ (mp 306°C) in the first, and between KCNS (mp 176°C) and HCOOK (mp 169°C) in the second system was very little. Notwithstanding this, the crystallization areas of NaCNS and KCNS proved to be larger than those of NaNO$_3$ and HCOOK, respectively. The little difference in the melting temperatures was not sufficient to account for the large differences of the crystallization areas. We think the entropy change in the fusion and in the solid-solid transition (occurring in the temperature range investigated) affected the extent of the crystallization area. In fact, the sum of the melting and transition entropies (*3*) was 9.33 eu for NaCNS, 8.11 eu for NaNO$_3$, 7.73 eu for KCNS, and 6.84 eu for HCOOK and the crystallization area, in these cases, was larger for the salt that had a larger entropy of fusion and transition. This fact, which was not contrary to the principle of the maximum entropy, emphasized the probable existence of another element, besides the melting temperature, that affected the extent of the crystallization areas.

LITERATURE CITED

(1) Berchiesi, G., Cingolani, A., Leonesi, D., *Z. Naturforsch.*, **25a**, 1766 (1970).
(2) Blander, M., "Molten salts chemistry," p 284, Interscience New York, N. Y., 1964.
(3) Braghetti, M., Berchiesi, G., Annual Meeting, Chimica Inorganica, Abs. no. 101 (1969).
(4) Braghetti, M., Berchiesi, G., Franzosini, P., *Ric. Sci.*, **39**, 576 (1969).
(5) Braghetti, M., Leonesi, D., Franzosini, P., *ibid.*, **38**, 116 (1968).
(6) Cingolani, A., Berchiesi, G., Piantoni, G., *J. Chem. Eng. Data*, submitted 1971.
(7) Leonesi, D., Piantoni, G., Berchiesi, G., Franzosini, P., *Ric. Sci.*, **38**, 702 (1968).
(8) Ricci, J. E. "The phase rule and heterogeneous equilibrium," p 315 ff., Dover Publications, New York, N. Y., 1966.
(9) Sinistri, C., Franzosini, P., *Ric. Sci. Rend. Sez.*, A 33 (2), 449 (1963).
(10) Sinistri, C., Franzosini, P., Rolla, M., *ibid.*, A 35 (2), 681 (1965).
(11) Sokolov, N. M., *Zh. Obshch. Khim.*, **24**, 1150 (1954).

RECEIVED for review March 12, 1971. Accepted September 15, 1971.